Estimation of kurtosis in accelerated diffusion spectrum imaging using compressed sensing

J. I. Sperl[1], E. T. Tan[2], K. Khare[2], K. F. King[3], X. Tao[2], C. J. Hardy[2], L. Marinelli[2], and M. I. Menzel[1]
[1]GE Global Research, Garching, Germany, [2]GE Global Research, Niskayuna, NY, United States, [3]GE Healthcare, Waukesha, WI, United States

Introduction

While diffusion tensor imaging (DTI) provides angular information of diffusivity, diffusion spectrum imaging (DSI) [1] also provides radial information such as diffusional kurtosis [2], which characterizes the deviation from Gaussian diffusion. As DTI has already proven its significance for detecting traumatic brain injury (TBI) [3] and multiple sclerosis (MS) [4], diffusional kurtosis may provide added information to characterize these diseases.

Clinical investigation of kurtosis requires fast and robust fitting techniques to determine the elements of the fourth order three-dimensional (3D) kurtosis tensor. Because fully-sampled DSI may be impractical due to its long acquisition times, the acquired data may be undersampled with or without a subsequent compressed sensing (CS) reconstruction [5, 6, 7]. Both methods will affect the derived kurtosis. Finally, various derived scalar measures (DSMs) of kurtosis are required, which are intended to serve as surrogate markers for TBI and MS.

Methods

In a DSI experiment, the signal S is acquired with diffusion encoding $q \in \mathbf{R}^3$ located on a Cartesian N-cube and for b-values $b = q^{\mathrm{T}}q \le b_{max}$. With $n \in \mathbf{R}^3$ the unit direction of q, the kurtosis expansion of the Gaussian diffusion of the signal reads

$$S(b,n) = S_0 \exp\left(-b\sum_{i=1}^{3}\sum_{j=1}^{3} n_i n_j D_{ij} + \frac{1}{6} b^2 MD^2 \sum_{i=1}^{3}\sum_{j=1}^{3}\sum_{k=1}^{3}\sum_{l=1}^{3} n_i n_j n_k n_l W_{ijkl} \right)$$

with S_0 the signal for $b = 0$, D_{ij} the elements of the (symmetric) diffusion tensor, MD the mean diffusivity (i.e. the mean of the eigenvalues of the diffusion tensor), and W_{ijkl} the elements of the (symmetric) kurtosis tensor. The unknown tensor elements are determined by a two step approach based on the logarithm of the signal: In the first step, the diffusion tensor elements D_{ij} are fit using data samples with small range of b-values ($b \le b_d$) for which the kurtosis terms (which are quadratic in b) can be neglected. In the second step, the remaining parameters W_{ijkl} are found using a larger range of b-values ($b \le b_k$, $b_d < b_k$). Both steps are performed by a linear least squares approach using the pseudoinverse (PI) of the coefficient matrix. As an extension to this approach, linear constraints are incorporated to ensure the physical relevance of the fitting parameters. This includes the positive definiteness of the diffusion tensor (implemented by the linear diagonal dominance criterion) as well as the non-negativity of the kurtosis tensor term for all gradient directions n. Both linearly constrained tasks yield a quadratic program which is addressed by an *active set strategy* [8].

The derived diffusion and kurtosis tensors are used to compute several DSMs as described in the literature. This includes the computation of the parallel, orthogonal, and mean kurtosis (K_{mean}) as defined in *Hui et al.*[9], as well as the maximum, minimum, and average apparent kurtosis coefficient (AKC_{max}, AKC_{min}, AKC_{avg}) based on the D-eigenvalues, the Kelvin-eigenvalues (μ_{max}, μ_{min}), and the surface mean M_Z as defined in *Qi et al.* [10].

DSI experiments on healthy volunteers were performed using a 3T GE MR750 clinical MR scanner (GE Healthcare, Milwaukee, WI, USA), equipped with an 8 channel head coil (*TE =141 ms, TR = 3 s, 128x128, FOV = 25 cm, slice = 4 mm, ASSET R = 2, b_{max} = 10,000 s/mm²*). Fitting (b_d = *1,300* s/mm², b_k = 7,000 s/mm²) and DSM computation were performed for fully sampled 3D q-space with *N=11* (FS_{11}), for randomly Gaussian undersampled data with acceleration factor *R=4* for *N=11* and *N=17* (US_{11}, US_{17}), and for the same undersampled data reconstructed using compressed sensing (CS_{11}, CS_{17}).

Results

Fig. 1 shows the orthogonal kurtosis resulting from the fitting procedure. For the unconstrained fit (FS_{11} PI), the kurtosis computation failed for several pixels due to negative values. This effect was eradicated in the constrained fit (FS_{11} QP) providing a superior result. Using undersampled data yielded noisier results (US_{11} QP), as the number of samples used for the kurtosis fit was reduced (from 305 to 109). A larger sampling grid (US_{17} QP, 423 samples) improved fitting. CS reconstruction (CS_{11} QP and CS_{17} QP) provided smoother results with reduced kurtosis peaks.

Fig. 2 shows line profiles of the various DSMs for CS_{17} QP. The Kelvin-Eigenvalues (μ_{max}, μ_{min}) provided efficiently computable bounds for kurtosis. The exactly computed AKC incorporates additional information, while the various definitions of mean kurtosis (AKC_{avg}, M_Z, K_{mean}) yielded all similar results.

Discussion and Conclusion

For fitting the diffusion and kurtosis tensors in DSI, quadratic programming is faster and more robust than nonlinear methods or maximum likelihood approaches [11, 12]. Fitting undersampled data increases the noise in the DSMs as there are fewer data samples available. Using CS can compensate for that and thus significantly reduce scan time (CS_{11} vs. FS_{11}) or improve fitting quality (CS_{17} vs. FS_{11}).

The denoising properties of the CS reconstruction may reduce the Rician-distributed noise floor and thus improve signal quality, especially for high b-values. On the other hand, it remains to be seen whether CS reconstruction leads to a systematic underestimation of kurtosis.

The analyzed DSMs are all capable of characterizing kurtosis bounds or averages. Since they differ with respect to accuracy, computational cost and robustness, clinical studies are warranted to determine their potential as surrogate markers for TBI or MS.

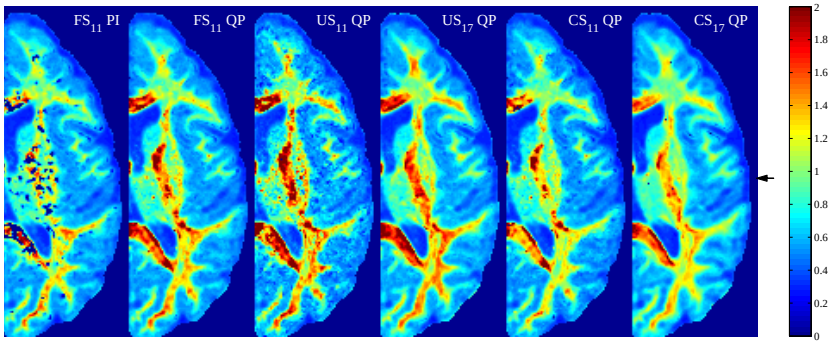

Fig. 1: Orthogonal kurtosis for different fits.

Fig. 2: Horizontal profile (indicated by the arrow in Fig. 1) of DSMs for CS_{17} QP.

References

[1] Wedeen VJ, Magn. Reson. Med., 2005
[2] Jensen JH *et al.*, Magn. Reson. Med. 2005
[3] Inglese M *et al.*, NMR Biomed. 2010
[4] Rovaris M *et al.*, Neurology 2005
[5] Donoho DL, IEEE Trans. Inform. Theory
[6] Khare K *et al.*, IEEE Trans. Med. Img., in review
[7] Menzel MI *et al.*, ISMRM 2010
[8] Bonnans JF and Lemaréchel C, Numerical Optimization, Springer, 2006
[9] Hui ES *et al.*, NeuroImage 2008
[10] Qi L *et al.*, J. Math. Anal. Appl., 2009
[11] Andersson JLR, NeuroImage, 2008
[12] Veraart J *et al.*, Magn. Reson. Med., 2010